Identification and vibrational properties of the mixed oxide $(1 - x)V_2O_5+xMoO_3$ $(x \leq 0.3)$

1992 J. Phys.: Condens. Matter 4 7377

(http://iopscience.iop.org/0953-8984/4/36/012)

J. Phys.: Condens. Matter 4 (1992) 7377–7388. Printed in the UK

Identification and vibrational properties of the mixed oxide $(1-x)V_2O_5 + xMoO_3$ ($x \leqslant 0.3$)

T Hirata† and Hai-Yan Zhu‡

† National Research Institute for Metals, 2-3-12, Nakameguro, Meguro-ku, Tokyo 153, Japan

‡ Zhejiang University, Hangzhou 310027, People's Republic of China

Received 2 December 1991, in final form 18 March 1992

Abstract. The mixed oxide $(1-x)V_2O_5 + xMoO_3$ ($x \leqslant 0.3$) has been synthesized by melting the oxides, and its structure and vibrational properties are investigated by x-ray diffractometry (XRD), x-ray photoelectron spectroscopy, Fourier transform infrared (IR) spectroscopy and Raman scattering. XRD revealed that the solid solutions of V_2O_5 with MoO_3 are well formed except that the second phase $V_9Mo_6O_{40}$ appeared at $x \geqslant 0.1$.

It turned out that the unit-cell dimension c of the solid solutions (orthorhombic) initially decreases whereas a and b increase with increasing x, and that all the lattice parameters tend to remain unchanged above $x \simeq 0.1$.

The IR band due to the V–O stretching vibration at 1028 cm^{-1} shifted downwards, diffused and decreased in intensity with increasing x; similar changes are observed in the Raman spectra of the mixed oxide. It is shown that the V valence transition from V^{5+} to V^{4+} occurs as V is replaced by Mo.

The V^{4+}-to-V^{5+} ratios obtained by deconvoluting the V $2p_{3/2}$ line showed some qualitative agreement with the prediction for $x < 0.1$ based on no Mo valence transition and the $V^{5+} \rightarrow V^{4+}$ transition as V is replaced by Mo.

It is concluded that the V valence transition is responsible for the vibrational property changes of the mixed oxide with x.

1. Introduction

Vanadium pentoxide V_2O_5 crystallizes in a layered structure (Bachmann *et al* 1961) and thereby is characterized by anisotropic physical properties. The vanadium in V_2O_5 exhibits a five square pyramidal coordination (Nabavi *et al* 1990) and alkali metal or hydrogen atoms can be incorporated between the layers to form bronzes, changing its structure as well as its physical properties (Tinet and Fripiat 1982, Tinet *et al* 1986). V_2O_5-based oxides have been extensively studied with respect to their catalytic activity (Ono *et al* 1984, Wachs and Chan 1984, Saleh *et al* 1986, Liu *et al* 1988a, b, 1989, Cristiani *et al* 1989, Ramirez *et al* 1990, Odriozola *et al* 1991) or electrochromism (Fujita *et al* 1985). From our viewpoint of the V_2O_5–MoO_3 system, however, there have been only a few studies of the mixed oxide $(1-x)V_2O_5+xMoO_3$ (Najbar and Niziol 1978, Liu *et al* 1989, Kang *et al* 1989), where the maximum solid solubility of MoO_3 in V_2O_5 amounts to 30 mol% according to the phase diagram (Robert *et al* 1981).

The vanadium in V_2O_5 is pentavalent (V^{5+}) whereas the molybdenum in MoO_3 is hexavalent (Mo^{6+}). Therefore, we may expect the V valence transition from V^{5+}

0953-8984/92/367377+12$04.50

to V^{4+} to occur when solid solutions of V_2O_5 with MoO_3 are formed, and it may be possible to determine the V^{4+}-to-V^{5+} ratio experimentally.

Meanwhile, it is expected that V–O bond lengths and angles change as a result of the V valence transition when V is replaced by Mo (Mo and V have different cation radii: $r_{Mo^{6+}} = 0.62$ Å and $r_{V^{5+}} = 0.54$ Å), leading to vibrational property changes of the mixed oxide.

The vibrational properties of K_xMoO_3 ($x = 0.1$–0.5) and $H_xV_2O_5$ ($x = 0$–3.27) have been investigated by Fourier transform (FT) infrared (IR) spectroscopy (Hirata and Yagisawa 1990, 1992).

Our attention is now directed towards understanding the structure and vibrational properties of the mixed oxide $(1-x)V_2O_5 + xMoO_3$ ($x \leqslant 0.3$).

This paper is organized as follows. In section 3.1, the structure of the mixed oxide is characterized by x-ray diffractometry (XRD). In sections 3.2 and 3.3, its vibrational properties are studied by FT IR spectroscopy and Raman scattering. In section 3.4, x-ray photoelectron spectroscopy (XPS) is performed to study the V valence transition from V^{5+} to V^{4+} in the mixed oxide. Finally, the structure and vibrational properties of the mixed oxide are discussed in section 4.

2. Experimental details

The mixed oxide $(1-x)V_2O_5 + xMoO_3$ ($x = 0.025$, 0.05, 0.10, 0.125, 0.15, 0.20, 0.25 and 0.30) was prepared by fusion of the oxides; appropriate amounts of two oxides, V_2O_5 and MoO_3, to give each value of x were taken, sealed in quartz tubes, melted at 700 °C (the melting point of V_2O_5 is about 690 °C), kept at that temperature for 1 h and cooled to room temperature (RT). No significant reaction of the melt with the quartz tubes occurred. The resultant products were annealed at 600 °C for 3 d in air to ensure their homogeneity and rapidly cooled to RT by taking them out of the furnace. The products changed colour from light green to deep green with increasing x whereas the colour of V_2O_5 is yellowish. X-ray diffractometry was performed with Cu Kα radiation to characterize the synthesized products, using Si as an internal standard. IR spectra were measured at RT with an FT IR spectrometer (JEOL 100), using a triglycine sulphate detector and KBr as reference between 400 and 4000 cm^{-1} or below 400 cm^{-1} with a resolution of 4 cm^{-1}. Raman scattering was performed on the pellets prepared from the pulverized products, by an FT–Raman spectrometer (JRS 5500N) with near-IR excitation (1064 nm). XPS was performed with a VG Scientific Escalab Mark II spectrometer using Mg Kα radiation (1233.6 eV). All measurements were made at a base pressure of less than 5×10^{-10} Torr in the analyser chamber.

3. Results

3.1. X-ray diffractometry

Figure 1 shows x-ray diffractograms of the mixed oxide $(1-x)V_2O_5 + xMoO_3$ ($0 < x \leqslant 0.3$) in two scattering angle regions: $2\theta = 29$–$35°$ in figure 1(i) and $2\theta = 39$–$45°$ in figure 1(ii); the x-ray diffractograms of V_2O_5 and MoO_3 are presented for comparison. These diffractograms reveal that the solid solutions of V_2O_5 with

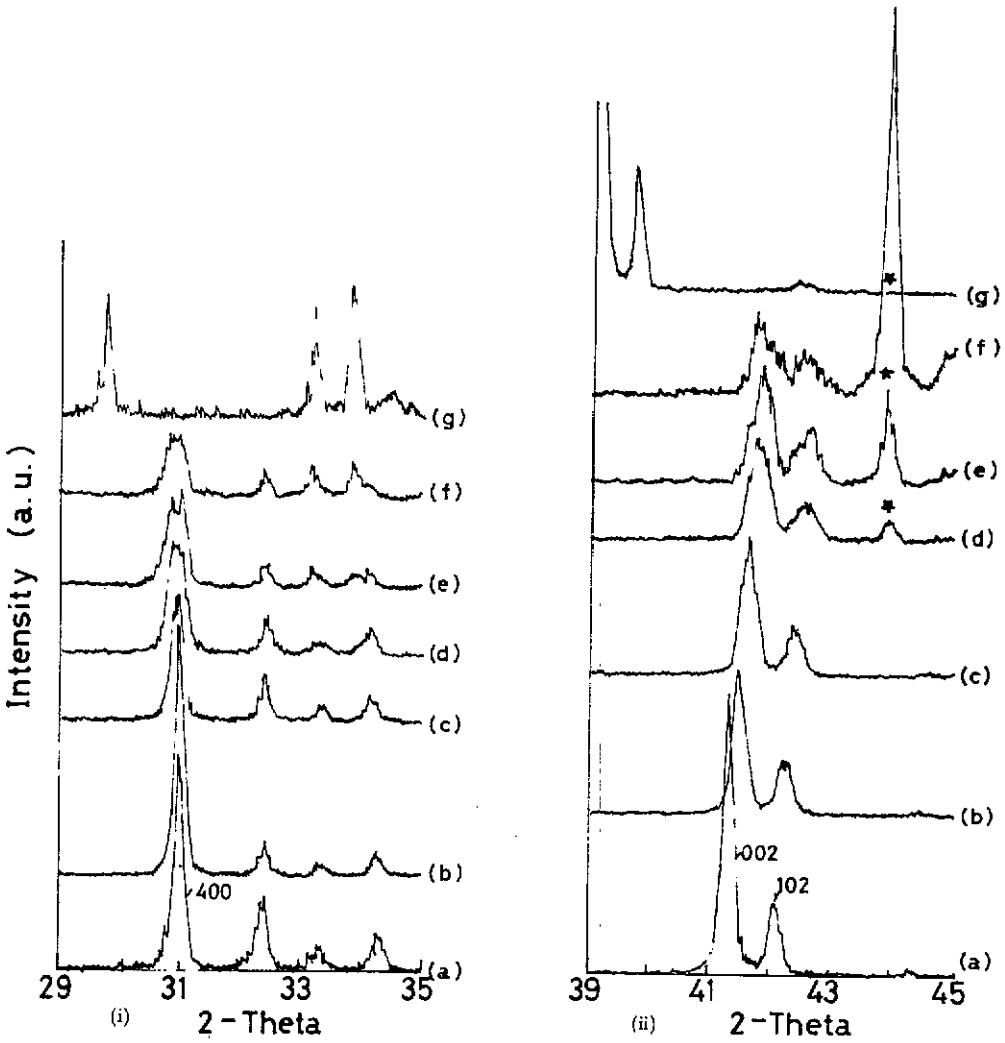

Figure 1. X-ray diffractograms of the mixed oxide $(1-x)V_2O_5 + xMoO_3$ between two different scattering angle regions (i) $2\theta = 29$–$35°$ and (ii) $2\theta = 39$–$45°$ (a.u., arbitrary units): curves (a), V_2O_5; curves (b), $x = 0.025$; curves (c), $x = 0.05$; curves (d), $x = 0.10$; curves (e), $x = 0.15$; curves (f), $x = 0.25$; curves (g), MoO_3.

MoO_3 are well formed by our sample preparation method, with evidence of no Bragg reflections associated with MoO_3 for the mixed oxide.

In figure 1, we can see that the (002) reflection for the mixed oxide (orthorhombic) clearly shifts to larger scattering angles with increasing x. Unit-cell dimensions of the mixed oxide are plotted as a function of x in figure 2 and are listed in table 1; they were determined by a least-squares refinement based on the setting of nine Bragg reflections using Si as an internal standard for the 2θ correction. Interplanar spacings or scattering angles of V_2O_5 and MoO_3 are in good agreement with those of the *Powder Diffraction File* (1984).

It is seen that c for the mixed oxide initially decreases whereas a and b increase

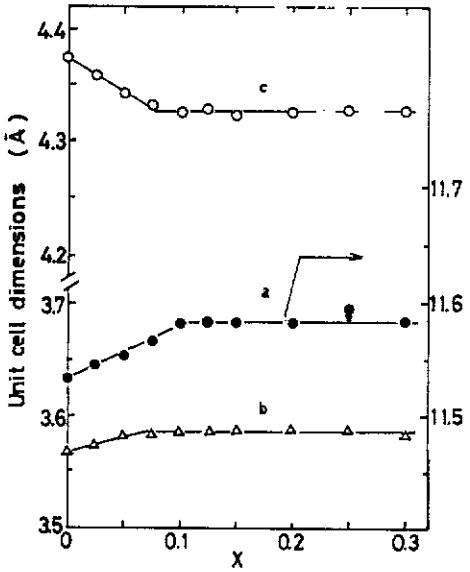

Figure 2. Plots of the unit-cell dimensions a, b and c as functions of x for the mixed oxide $(1-x)V_2O_5 + xMoO_3$.

Table 1. Unit-cell dimensions of the mixed oxide $(1-x)V_2O_5 + xMoO_3$.

x	a (Å)	b (Å)	c (Å)
0(V_2O_5)	11.532	3.567	4.373
0.025	11.545	3.572	4.358
0.05	11.555	3.582	4.342
0.075	11.566	3.583	4.433
0.10	11.585	3.585	4.326
0.125	11.583	3.585	4.328
0.15	11.583	3.587	4.322
0.20	11.584	3.588	4.326
0.25	11.596	3.587	4.327
0.30	11.584	3.582	4.329

with increasing x. It is interesting to note that all the unit-cell dimensions tend to remain unchanged above $x \simeq 0.1$.

A few lines appeared in the x-ray diffractograms of the mixed oxide with $x \geqslant 0.10$, and their intensities increased with further increase in x (see, for example, the peaks labelled with a star in figure 1(ii)). They could be assigned to a vanadium molybdenum oxide $V_9Mo_6O_{40}$ (Joint Committee on Powder Diffraction Standards 1989) (orthorhombic) in the V_2O_5–MoO_3 system (Munch and Pierron 1964, Bielanski and Najibar 1978).

The tendency for the unit-cell dimensions to remain unchanged at $x \gg 0.1$ is relevant to the precipitation of $V_9Mo_6O_{40}$ in the solid solutions. Quenching from the solid-solution region (600 °C) did not avoid the formation of $V_9Mo_6O_{40}$ for the mixed oxide with $x \geqslant 0.10$. It is considered that the solvus line is really ambiguous in the phase diagram proposed for the V_2O_5–MoO_3 system (Bielanski and Najibar 1978).

3.2. Infrared spectroscopy

Figure 3 shows IR spectra of the mixed oxide; for comparison, IR spectra of V_2O_5 as well as MoO_3 are shown too. The spectrum of V_2O_5 is in good agreement with that in the literature. The band at 1028 cm^{-1} and the broad band at around 823 cm^{-1} are assigned to the stretching vibration of the V–O group and the deformation vibration of V–O–V bridges (Frederickson and Hausen 1963, Dickens *et al* 1984, Cristiani *et al* 1989, Ramirez *et al* 1990). Similarly, the bands at 999 cm^{-1} and 820 cm^{-1} in the spectrum of MoO_3 are due to the Mo–O stretching vibration and the Mo–O–Mo bridging vibration, respectively (Beattie *et al* 1971, Razl Seyedmonlr *et al* 1982). We notice that the V–O stretching vibration mode decreases in intensity and becomes diffuse with increasing x. It is evident that this mode shifts downwards with increasing x as seen from the expanded representation in figure 4; the frequency change of this mode has been cited with regard to the activity and selectivity of the V_2O_5–MoO_3 catalyst (Hair 1967).

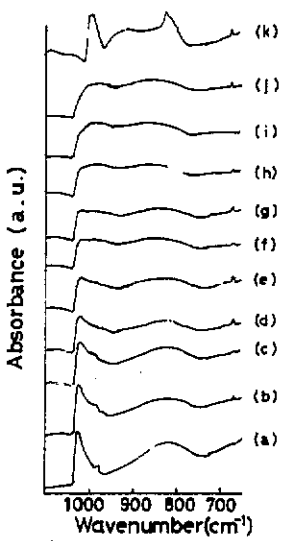

Figure 3. IR spectra between 650 and 1100 cm^{-1} for the mixed oxide $(1-x)V_2O_5 + xMoO_3$ (a.u., arbitrary units): curve (a), V_2O_5; curve (b), $x = 0.025$; curve (c), $x = 0.05$; curve (d), $x = 0.075$; curve (e), $x = 0.10$; curve (f), $x = 0.125$; curve (g), $x = 0.15$; curve (h), $x = 0.20$; curve (i), $x = 0.25$; curve (j), $x = 0.30$; curve (k), MoO_3.

The frequency of the V–O stretching vibration mode decreases linearly with increasing x, as shown in figure 5. It was difficult to determine the exact frequency for the mixed oxide with $x \geqslant 0.15$ because of broad peaks. The frequency of the Raman band at 997 cm^{-1} was carefully searched for on an expanded spectrum on the CRT, which also showed a linear decrease with increasing x (figure 5).

In order to obtain any information concerning the distortions of edge-sharing VO_5 polyhedra as V is replaced by Mo, an attempt has been made to measure far-IR spectra. Figure 6 represents far-IR spectra of the mixed oxide $(1-x)V_2O_5 + xMoO_3$ ($x = 0.025$, $x = 0.075$ and $x = 0.15$) together with those of V_2O_5 as well as MoO_3, for comparison. Two IR bands at 316 and 386 cm^{-1} in the far-IR spectrum of V_2O_5 are assigned to the angular deformation mode (δ V–O–V) related to the V–O bonds (Nabavi *et al* 1991); the triple bands at 351, 360 and 375 cm^{-1} for MoO_3 are assigned to the B_u mode (Beattie *et al* 1971). It is shown that the bands labelled A and B decrease in intensity and become diffuse with increasing x. In addition, band A

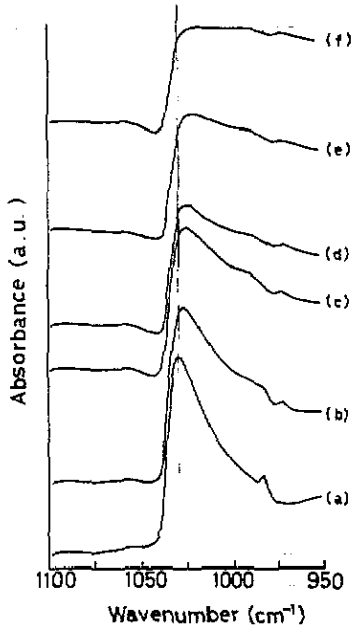

Figure 4. The expanded representation to demonstrate the downward shift of the V–O stretching vibration mode with x (a.u., arbitrary units): curve (a), V_2O_5; curve (b), $x = 0.025$; curve (c), $x = 0.05$; curve (d), $x = 0.075$; curve (e), $x = 0.10$; curve (f), $x = 0.125$.

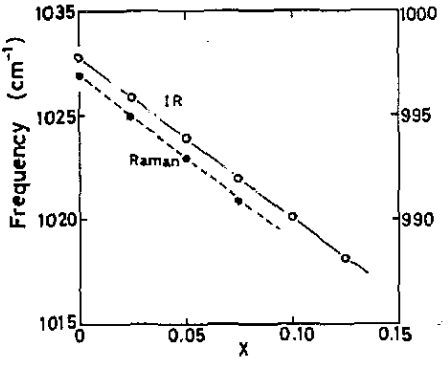

Figure 5. Frequency shift of the IR band at 1028 cm^{-1} ($x = 0$) with x for the mixed oxide $(1 - x)V_2O_5 + xMoO_3$; the frequency shift of the Raman band at 997 cm^{-1} ($x = 0$) is also plotted. The left-hand scale is for the IR data and the right-hand is for the Raman data.

shifts upwards and tends to merge into band B with increasing x. It is considered that these spectral changes are associated with the perturbation of the linkage between the edge-sharing VO_5 polyhedra which influences the angular deformation mode as V is replaced by Mo (Nabavi *et al* 1991). No direct relation to the far-IR spectrum of MoO_3 could be given.

3.3. Raman spectroscopy

Figure 7(i) shows the Raman spectra of V_2O_5 and MoO_3. The Raman spectra of the mixed oxide $(1 - x)V_2O_5 + xMoO_3$ with $x = 0.025$, $x = 0.05$ and $x = 0.075$ are given in figure 7(ii). The Raman spectrum of MoO_3 is in good agreement with the previous data (Razl Seyedmonlr *et al* 1982, Mohan and Ravikumar 1983). The bands at 997 and 821 cm^{-1} are assigned to the Mo–O symmetric and asymmetric

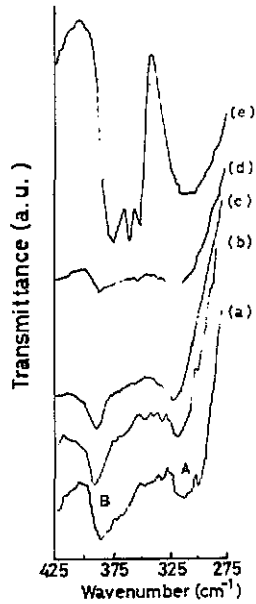

Figure 6. Far-IR spectra between 300 and 500 cm^{-1} for the mixed oxide $(1-x)V_2O_5 + xMoO_3$ (a.u., arbitrary units): curve (a), V_2O_5; curve (b), $x = 0.025$; curve (c), $x = 0.075$; curve (d), $x = 0.15$. For comparison, the far-IR spectrum of MoO_3 (curve (e)) is shown as well.

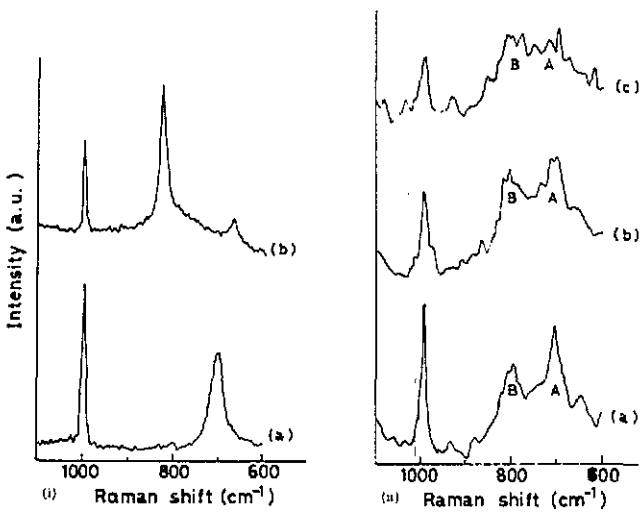

Figure 7. Raman spectra of (i) V_2O_5 (curve (a)) and MoO_3 (curve (b)) and (ii) the mixed oxide $(1-x)V_2O_5 + xMoO_3$ with $x = 0.025$ (curve (a)), $x = 0.05$ (curve (b)) and $x = 0.075$ (curve (c)) (a.u., arbitrary units).

stretching vibrations, respectively; the small band at 667 cm^{-1} is due to the second-order Raman scattering, i.e. the subtraction of the O–Mo–O asymmetric bending vibration (335 cm^{-1}) from the Mo–O symmetric stretching vibration gives rise to this small band. The Raman spectrum of V_2O_5 also coincides well with those given in the literature (Beattie and Gilson 1968, 1969, Wachs and Chan 1984, Cristiani *et al* 1989, Saleh *et al* 1986).

The bands at 997 cm^{-1} and 700 cm^{-1} are assigned to the V–O symmetric and

asymmetric stretching vibrations, respectively. For the mixed oxide, the Raman band at 997 cm^{-1} shifts downwards and decreases in intensity with increasing x, increasing the full width at half-maximum (FWHM); the frequency of this Raman band which was determined on an expanded spectrum on the CRT is presented in figure 5. The two Raman bands A and B decrease in intensity and become broader with increasing x. We note that the frequency of band B does not exactly correspond to that of the band at 821 cm^{-1} for MoO_3; this band could be assigned to the Mo–O vibration in the mixed oxide.

Raman spectroscopy indicates the formation of polyhedra with bond lengths and angles different from those in V_2O_5, reflecting the structural distortions as MoO_3 is intercalated into V_2O_5.

3.4. XPS

Figure 8 shows the V 2p core-level spectra including the O 1s line for the mixed oxide; the spectrum of V_2O_5 is shown as well. The spectra for all the different x-values are not presented since some spectra are almost the same as those in figure 8. The binding energies were corrected with reference to the O 1s line at 529.48 eV. The spectrum of V_2O_5 is in good agreement with the previous data (Fujita *et al* 1985, Haber *et al* 1985, Liu *et al* 1988a, b, Khawaja *et al* 1989, Odriozola *et al* 1991).

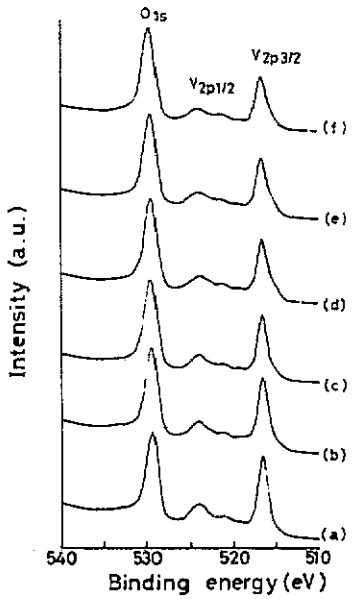

Figure 8. V 2p core-level spectra of the mixed oxide $(1-x)V_2O_5+xMoO_3$ (a.u., arbitrary units): curve (a), V_2O_5; curve (b) $x = 0.025$; curve (c), $x = 0.05$; curve (d), $x = 0.10$; curve (e), $x = 0.15$; curve (f), $x = 0.25$.

It is of particular interest to note that the V $2p_{3/2}$ line decreases in intensity with increasing x, and that a small peak tends to appear at the foot shifted by about 1 eV from the predominant V $2p_{3/2}$ line at 516.6 eV. These spectral changes suggest the V valence transition from V^{5+} to V^{4+} as reported for the vanadium species in the 4+ oxidation state (Haber *et al* 1985, Odriozola *et al* 1991).

An attempt was made to estimate the V^{4+}-to-V^{5+} ratio by deconvoluting the V $2p_{3/2}$ line with two Gaussian and/or Lorentzian curves of FWHM 1.4 eV or less,

separated by 1 eV (Yan and Anderson 1991) with or without a background and satellite subtraction; both yielded similar results for the V^{4+}-to-V^{5+} ratio. However, our deconvolution yielded a V^{4+}-to-V^{5+} ratio of 4% even for V_2O_5, which is an order of magnitude larger than that determined by ESR spectroscopy (Tanabe *et al* 1978). Thus, this ratio for V_2O_5 was subtracted as a correction from the V^{4+}-to-V^{5+} ratios for the mixed oxide.

Figure 9 shows a representative deconvolution for the V $2p_{3/2}$ line of the mixed oxide with $x = 0.25$.

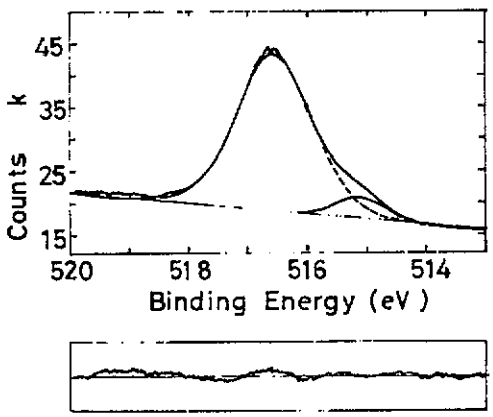

Figure 9. A representative deconvolution for the V $2p_{3/2}$ line of the mixed oxide with $x = 0.25$.

In figure 10, the V^{4+}-to-V^{5+} ratios are plotted as a function of x for the mixed oxide, compared with the prediction according to

$$(1-x)V_2O_5+xMoO_3-(x/2)O = xMo^{6+}+5(1-x/2)O+(2-3x)V^5+xV^{4+}. \tag{1}$$

This equation can be derived on the basis that V is partly transformed to V^{4+} and the rest of V remains pentavalent as V is replaced by Mo on the condition that the Mo valence does not change. Equation (1) meets the condition for charge neutrality as well as the condition that the total number of V^{5+} and V^{4+} equals $2(1-x)$. It is proved that no Mo valence transition occurs as there is no Mo 3d core-level spectral change with respect to the binding energies and lineshapes for the mixed oxide.

We can see that the experimental V^{4+}-to-V^{5+} ratios increase in qualitative agreement with the prediction up to $x = 0.1$ and then tend to decrease or level off with further increasing x. We also tried to obtain the V^{4+}-to-V^{5+} ratios from the difference spectrum between the V $2p_{3/2}$ core-level spectra of V_2O_5 and the mixed oxide. Quite a similar trend to that shown in figure 10 was observed.

4. Discussion

First, we should recall that the V–O stretching vibration mode along the c axis of the mixed oxide shifts downwards with increasing x. This contradicts the decrease in c with increasing x, in view of the generally accepted rule that shorter bond lengths

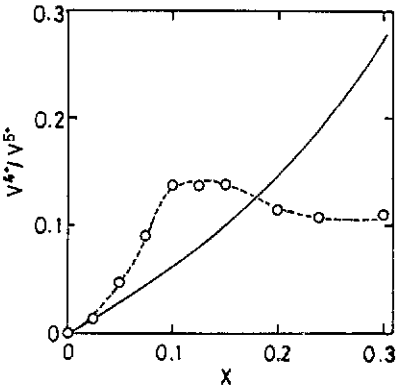

Figure 10. Plot of the V^{4+}-to-V^{5+} ratios as a function of x for the mixed oxide $(1-x)V_2O_5 + xMoO_3$; – – –, guide to the eye; ○, experiments; ——, prediction according to equation (1).

correspond to high force constants, leading to a hardening of vibration modes. The mode Grüneisen parameter γ is defined as $\gamma(\omega) = \mathrm{d}(\ln \omega)/3\mathrm{d}(\ln c)$, where c represents the unit-cell dimension along the direction of vibration. Taking account of the linear decrease in c with increasing x for $x < 0.1$ and $\mathrm{d}\omega/\mathrm{d}x \simeq 77$ cm^{-1} (see figures 2 and 5), we find an anomalous sign (negative) for γ. This requires us to tackle the problem on the basis of the bond-length changes in the internal coordinates of the unit cell.

We consider that the short bond distance of V–O (1.54 Å) along the c axis in V_2O_5 increases whereas the long bond distance of V–O (about 2.78 Å) decreases even more with increasing x, leading to an actual decrease in the lattice constant c. The opposite bond-length changes along the c axis have been proposed for $YBa_2Cu_3O_{7-y}$, where the Cu(1)–O(1) bond length decreases with increasing oxygen deficiency whereas the Cu(2)–O(1) bond length increases (Kourouklis *et al* 1987), resulting in the actual expansion of the c axis.

It is considered that the fact that the ion radii of V^{4+} and/or Mo^{6+} are larger than that of V^{5+} could be responsible for the increase in the bond length of V–O. The substitution of Mo^{6+} for V^{5+} causes the $V^{5+} \rightarrow V^{4+}$ transition, which results in an increase in the bond length of V–O (1.54 Å) and a decrease in the bond length of V–O (2.78 Å) along the c axis. In fact, the lower the oxidation state of V, the longer the V–O bond length becomes (Ramirez *et al* 1990). Thus, we can consider that the V–O bond length increases when the V valence changes from V^{5+} to V^{4+} as V is replaced by Mo, and we expect a softening of the vibration mode in question.

It is ruled out that the downward shift of the V–O stretching vibration mode with increasing x is due to a mass-change-induced effect. The frequency shift based on the mass change is equal to $\omega_{V_{Mo}}/\omega_V = (m_V/m_{V_{Mo}})^{1/2}$, where m_V and $m_{V_{Mo}}$, respectively, represent the masses of V before and after V has been replaced by Mo, and $m_{V_{Mo}}$ is given by $(1-x)m_V + xm_{Mo}$. This yields too large a frequency shift to reconcile with the experiments; for example, $(m_V/m_{V_{Mo}})^{1/2} \simeq 0.98$ even for the mixed oxide with $x = 0.025$.

The decrease in intensity of the IR band at 1028 cm^{-1} with increasing x is also ascribed to the $V^{5+} \rightarrow V^{4+}$ transition. The intensity of the IR band is proportional to

the effective charge (Brodsky *et al* 1977) and, the greater the ionization potential, the larger the effective charge becomes. Since the ionization potential of V^{5+} is greater than that of V^{4+}, the $V^{5+} \rightarrow V^{4+}$ transition causes a decrease in the intensity of the IR band. With respect to the Raman band at 997 cm^{-1}, it should be noted that this Raman band is unique to V_2O_5 and is absent in vanadium oxides in lower oxidation states of V (Wachs and Chan 1984). Consequently, the decrease in intensity of the Raman band is also associated with the $V^{5+} \rightarrow V^{4+}$ transition.

The V valence transition from V^{5+} to V^{4+} as V is replaced by Mo is confirmed by XPS. Our experimental V^{4+}-to-V^{5+} ratios are qualitatively in line with the prediction according to equation (1) for $x < 0.1$. While we can state that XPS is only qualitative when the V^{4+}-to-V^{5+} ratio is much less than about 0.1, another possible reason for this imperfect agreement is that the fixed oxygen content may not be retained because of oxygen deficiency or excess in the mixed oxide. For $x > 0.1$, the deviation from the prediction tends to be significant; this could be attributed to the existence of the second phase $V_9Mo_6O_{40}$ where all the vanadium is not in the oxidation state of V^{5+} but in the mixed oxidation states V^{4+} and V^{5+} with a V^{4+}-to-V^{5+} ratio of $\frac{1}{8}$. It is noticed that the changing trend in the V^{4+} component with x is quite similar to that determined by a chemical method (Tanabe *et al* 1978). Complementary work to determine the V^{4+} component in the mixed oxide by ESR spectrsocopy is in progress. Fujita *et al* (1985) have reported that V_2O_5 changes colour from yellow to green when VO_2 (V^{4+}) is formed. This colour change corresponds to what we have observed for the mixed oxide.

Summing up, the mixed oxide $(1-x)V_2O_5 + xMoO_3$ undergoes the V valence transition from V^{5+} to V^{4+} as V is replaced by Mo; this was confirmed by XPS. This valence transition is responsible for the vibrational property changes of the mixed oxide as observed by IR spectroscopy and Raman scattering. Finally, we would like to comment that the solid-solution region in the V_2O_5–MoO_3 system is much narrower than in the proposed phase diagram.

Acknowledgments

We thank Dr K Yagisawa for his critical comments. Thanks are also due to Dr K Kawauchi of JEOL Ltd for the Raman scattering measurements. One of the authors (Hai-Yan Zhu) benefitted from a fellowship of the Science and Technology Agency of the Japanese Government.

References

Bachmann H G, Ahmed F R and Barnes W H 1961 *Z. Kristallogr. Kristallgeom.* **115** 110
Beattie I R, Cheetham N, Gardner M and Rogers D E 1971 *J. Chem. Soc.* A 220
Beattie I R and Gilson T R 1968 *Proc. R. Soc.* A **307** 407
—— 1969 *J. Chem. Soc.* A 2322
Bielanski A and Najibar N 1978 *Pol. J. Chem.* **52** 883
Brodsky M H, Cardona M and Cuomo J J 1977 *Phys. Rev.* B **16** 3556
Cristiani C, Forzatti P and Busca G 1989 *J. Catal.* **116** 586
Dickens P G, Chippindale A M, Hibble S J and Lancaster P 1984 *Mater. Res. Bull.* **19** 319
Frederickson L D and Hausen D M 1963 *Anal. Chem.* **35** 818
Fujita F, Miyazaki K and Tatsuyama C 1985 *Japan. J. Appl. Phys.* **24** 1082
Haber J, Machej T and Czeppe T 1985 *Surf. Sci.* **151** 301

Hair M L 1967 *Infrared Spectroscopy in Surface Chemistry* (New York: Dekker) p 212
Hirata T and Yagisawa K 1990 *J. Phys.: Condens. Matter* **2** 5199
—— 1992 *J. Alloys Compounds* **185** 177
Joint Committee on Powder Diffraction Standards 1989 *Powder Diffraction File* (Swarthmore, PA: International Center for Diffraction Data) card 34-527
Kang Z C, Bao Q X and Boulesteix C 1989 *J. Solid State Chem.* **83** 255
Khawaja E E, Salim M A, Khan M A, Al-Adel F F, Khattak G D and Hussain Z 1989 *J. Non-Cryst. Solids* **110** 33
Kourouklis G A, Jayaraman A, Batlogg B, Cava R J, Stavola M, Krol D M, Rietman E A and Schneemeyer L F 1987 *Phys. Rev.* B **36** 8320
Liu Z X, Bao Q X and Wu N J 1988a *J. Catal.* **113** 45
Liu Z X, Lin Z D, Fan H, Li F H, Bao Q X and Zhang S 1988b *Appl. Phys.* A **45** 159
Liu Z X, Xie K, Li Y Q and Bao Q X 1989 *J. Catal.* **119** 249
Mohan S and Ravikumar K G 1983 *Bull. Soc. Chim. Fr.* **11–2** 267
Munch R H and Pierron E 1964 *J. Catal.* **3** 406
Nabavi M, Sanchez C and Livage J 1991 *Phil. Mag.* B **63** 941
Nabavi M, Taulelle F, Sanchez C and Verdaguer M 1990 *J. Phys. Chem. Solids* **51** 1375
Najbar M and Niziol S 1978 *J. Solid State Chem.* **26** 339
Odriozola J A, Soria J, Somorjai G A, Heinemann H, Carcia de la Banda J F, Lopez Grandos M and Conesa J C 1991 *J. Phys. Chem.* **95** 240
Ono T, Nakagawa Y, Miyata H and Kubokawa Y 1984 *Bull. Chem. Soc. Japan* **57** 1205
Powder Diffraction File 1984 (Swarthmore: International Center for Diffraction Data) cards 9-387 and 5-508
Ramirez R, Casal B, Utrera L and Ruiz-Hitzky E 1990 *J. Phys. Chem.* **94** 8960
Razi Seyedmonir S, Abdo S and Howe Russell F 1982 *J. Phys. Chem.* **86** 1233
Roth Robert S, Negas T and Cook L P 1981 *Phase Diagrams for Ceramists* vol IV, (Columbus, OH: American Ceramic Society) p 47
Saleh R Y, Wachs I E, Chan S S and Chersich C C 1986 *J. Catal.* **98** 102
Tanabe K, Seiyama T and Fueki K (ed) 1978 *Metal Oxides and Mixed Oxides* (Tokyo: Kodansha) p 338 (in Japanese)
Tinet D and Fripiat J J 1982 *Rev. Chim. Minéral.* **19** 612
Tinet D, Legay M H, Gatineau L and Fripiat J J 1986 *J. Phys. Chem.* **90** 948
Wachs I E and Chan S S 1984 *Appl. Surf. Sci.* **20** 181
Yan Z G and Anderson S Lars T 1991 *J. Catal.* **131** 350